Reactions of Laser-Ablated Rhodium Atoms with O_2. Infrared Spectra and DFT Calculations for RhO, ORhO, $(O_2)RhO_2$, Rh_2O_2, $Rh(O_2)$ and $(O_2)Rh(O_2)$ in Solid Argon

Angelo Citra and Lester Andrews*

Department of Chemistry, University of Virginia, Charlottesville, Virginia 22901

Received: March 11, 1999; In Final Form: April 23, 1999

Laser-ablated Rh atoms react to give RhO, the linear dioxide ORhO, the side-bound dioxygen adduct $(O_2)RhO_2$, and several $ORhO(O_2)$ complexes. In addition, a large number of $Rh_x(O_2)_y$ complexes are observed, but only $Rh(O_2)$ and $(O_2)Rh(O_2)$ can be identified with the support of DFT frequency calculations. These calculations also characterize $(O_2)RhO_2$ as a peroxide with rhodium approaching the +6 oxidation state and $(O_2)Rh(O_2)$ between a disuperoxo and diperoxo species. Comparisons among the Co, Rh, and Ir dioxygen systems are given.

Introduction

The interactions between transition metal atoms and dioxygen are of interest in a biological context,[1,2] and there are several examples of rhodium superoxo complexes.[3−5] Furthermore, dioxygen complexes of Rh^{II} porphyrins are related to the isoelectronic Co^{II} compounds, except that the enhanced covalent-bond formation in the second transition series results in greater stability for the rhodium−dioxygen complexes.[4] The catalytic behavior of supported rhodium where a dioxygen complex oxidizes carbon monoxide is also important,[6] as the common auto exhaust catalytic converter employs rhodium deposited on a mesh of alumina. Transition metal oxygen complexes function as oxygen transfer agents to organic substrates.[7] Rhodium peroxo species have been shown to act as reactive intermediates in the transformation of terminal alkenes to methyl ketones and to oxidize cyclohexenes to give several products, including the epoxide.[8] It is also significant to note that rhodium clusters are receiving considerable attention owing to their magnetic behavior as a function of cluster size, particularly in view of the nonmagnetic behavior of the bulk solid.[9,10]

In this study rhodium atoms produced by laser ablation of a rhodium target are reacted with dioxygen in an argon stream and the products are trapped at cryogenic temperatures. Annealing cycles allow controlled diffusion and reaction of the isolated species. This maximizes the interaction between rhodium and oxygen and shows the full extent of their chemistry under extreme conditions. The reaction of thermally generated rhodium atoms and dioxygen has been studied in inert matrixes previously, and numerous rhodium dioxygen species were identified;[11,12] however, many of these assignments are incorrect, as thermal rhodium atoms are much more reactive than anticipated. The results of the present work are discussed within the context of the cobalt and iridium dioxygen systems, which have already been studied in this laboratory,[13,14] and comparisons between the three systems are made.

Experimental Section

The technique for laser ablation and FTIR matrix investigation has been described previously.[15,16] Rhodium metal (Goodfellow Metals) was mounted on a rotating (1 rpm) stainless steel rod. The Nd:YAG laser fundamental (1064 nm, 10 Hz repetition rate, 10 ns pulse width, 40−50 mJ pulses) was focused on the target through a hole in the CsI cryogenic window (maintained at 7−8 K). Metal atoms were co-deposited with 1% O_2 ($^{16}O_2$, $^{18}O_2$, $^{16,18}O_2$, and mixtures) in argon at 5−8 mmol/h for 1−2 h periods. FTIR spectra were recorded with 0.5 cm^{-1} resolution on a Nicolet 550 spectrometer. Matrix samples were successively warmed and recooled, and more spectra were collected; the matrix was subjected to broad-band photolysis with a medium-pressure mercury arc (Philips, 175 W, globe removed, 240−580 nm) at different stages in the annealing cycles.

Results

Infrared spectra and density functional theory calculations of rhodium−oxygen reaction products will be presented. Infrared spectra in the 1740−1680 cm^{-1}, 1380−1020 cm^{-1} and 960−800 cm^{-1} regions for $^{16}O_2$ are shown in Figures 1 and 2 for 0.6% O_2; at the final annealing temperature attained, 47 K, argon sublimation was noticed and the temperature was quickly dropped back to 7−8 K. Infrared spectra in the 580−440 cm^{-1} region for $^{16}O_2$, $^{18}O_2$, mixed $^{16}O_2+^{18}O_2$, and scrambled $^{16}O_2+^{16}O^{18}O+^{18}O_2$ are illustrated in Figure 2. The spectra obtained using isotopically scrambled oxygen in the important metal oxide stretching region are shown in Figure 4. All absorptions and isotopic counterparts are listed in Table 1.

Density functional theory (DFT) calculations using the Gaussian 94 program[17] were employed to calculate structures and frequencies for rhodium oxide product molecules to verify assignments and to provide information on their ground-state properties. The BPW91 density functional D95* basis set for oxygen and Los Alamos ECP plus DZ basis set for rhodium were used.[18−20] The calculated geometries, relative energies, frequencies, and vibrational analyses are given in Tables 2−5 and in Figure 5.

Discussion

New rhodium oxide species will be identified from isotopic shifts and DFT calculations.

RhO. A band is observed at 799.0 cm^{-1} after initial deposition which shows a marginal increase on photolysis on early annealing but decreases in intensity on higher annealing. The $^{18}O_2$ counterpart for this band is at 759.8 cm^{-1} giving an

10.1021/jp990864a CCC: $18.00
Published on Web 06/06/1999

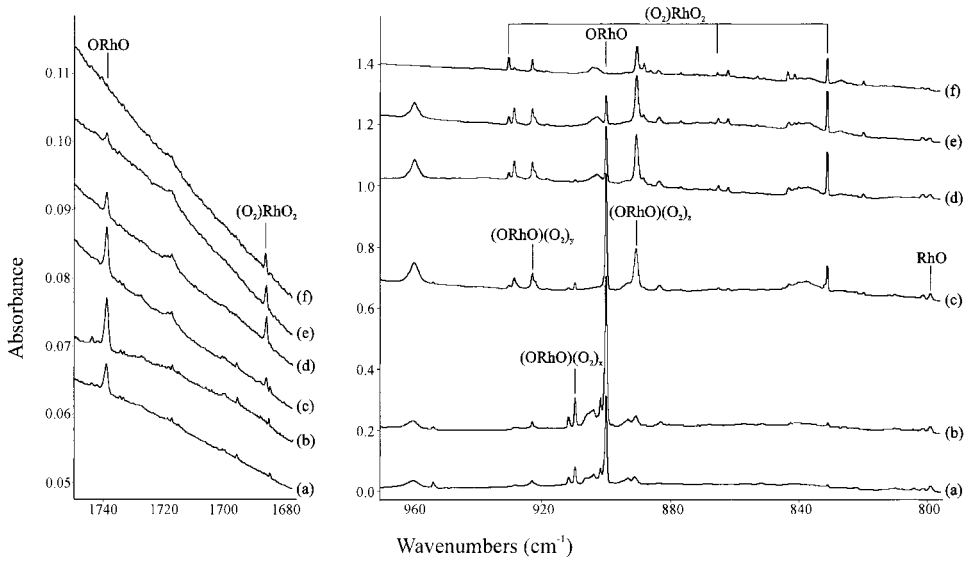

Figure 1. Infrared spectra in the 1750−1680 cm^{-1} and 970−800 cm^{-1} regions for laser-ablated rhodium atoms co-deposited with oxygen (0.6%) in argon on a 7−8 K window: (a) after 2 h deposition, (b) after broad-band photolysis for 20 min, (c) after annealing to 25 K, (d) after annealing to 35 K, (e) after annealing to 40 K, and (f) after annealing to 47 K.

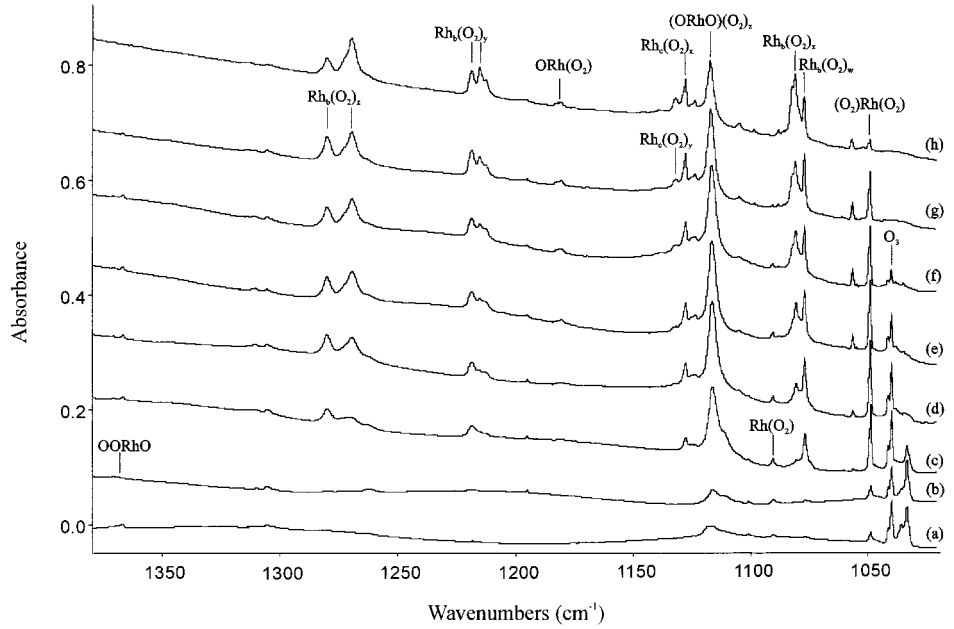

Figure 2. Infrared spectra in the 1380−1020 cm^{-1} region for laser-ablated rhodium atoms co-deposited with oxygen (0.6%) in argon on a 7−8 K window: (a) after 2 h deposition, (b) after broad-band photolysis for 20 min, (c) after annealing to 25 K, (d) after annealing to 30 K, (e) after annealing to 35 K, (f) after annealing to 40 K, (g) after annealing to 45 K, and (h) after annealing to 47 K.

isotopic ratio of 1.05159, only slightly smaller than the harmonic diatomic ratio of 1.05185. No intermediate bands are observed in either the mixed ($^{16}O_2$+$^{18}O_2$) or scrambled ($^{16}O_2$+$^{16}O^{18}O$+$^{18}O_2$) isotopic experiment, indicating that only one oxygen atom is involved in this vibration. The isotopic doublet and ratio support the assignment of this band to the diatomic molecule RhO. The small discrepancy in the isotopic ratio can be attributed to normal cubic anharmonicity.

DFT calculations for the doublet, quartet, and sextet states of RhO have been performed and the results are summarized in Tables 2 and 3. The $^4\Sigma^-$ state is found to lie lowest, and the calculated frequency of 838.3 cm^{-1} is in good agreement with the experimental value. The scale factor, 0.953, is lower than scale factors reported for transition metal compounds and similar calculations.[21] The doublet state is calculated to be 30 kJ/mol higher in energy. Earlier calculations[22] also predicted a $^4\Sigma^-$ ground state, but UHF obtained an unreasonably low 519 cm^{-1} frequency.[22b] Early experimental work reported RhO in emission and mass spectra.[23] A preliminary analysis of the dispersed $^4\Pi \rightarrow {}^4\Sigma^-$ fluorescence spectrum[24] from work in progress finds the ground-state RhO vibrational frequency 785 ± 10 cm^{-1}, which is in excellent agreement with the present work. A very recent photoelectron spectrum finds a 730 ± 80 cm^{-1} frequency for ground state $^4\Sigma^-_{3/2}$ RhO.[25]

ORhO. The sharp intense band at 900.1 cm^{-1} after initial deposition doubles in absorbance on photolysis but decreases on annealing (Figure 1). The $^{18}O_2$ counterpart for this band at 861.3 cm^{-1} gives an isotopic ratio of 1.04505, much lower than the harmonic diatomic value of 1.05185, but only slightly lower than the harmonic value 1.04539 for the antisymmetric stretching mode ν_3 of a linear ORhO molecule. No intermediate peaks are observed in the mixed isotopic experiment, but a triplet of

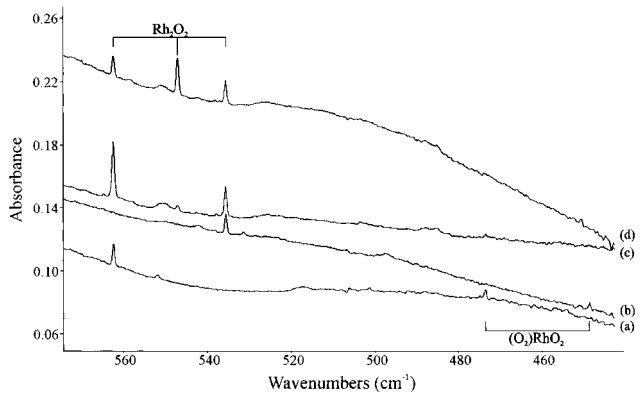

Figure 3. Infrared spectra in the 570−440 cm^{-1} region after annealing to 30 K: (a) $^{16}O_2$, (b) $^{18}O_2$, (c) $^{16}O_2+^{18}O_2$, and (d) $^{16}O_2+^{16}O^{18}O+^{18}O_2$.

peaks is observed in the scrambled isotopic experiment, the intermediate peak occurring at 888.0 cm^{-1} with approximately 1.3 times the intensity of the pure isotope bands. The low ratio, unusual relative intensities, and marked asymmetry in the scrambled isotopic triplet are analogous to OIrO which exhibited the same behavior,[14] and the 900.1 cm^{-1} band is assigned to the ν_3 mode of ORhO. The isotopic ratio can be used to estimate the bond angle,[26] and the molecule is found to be linear, in agreement with an earlier ESR study.[27] The band due to the mixed isotopic molecule $^{16}ORh^{18}O$ lies 7.3 cm^{-1} above the midpoint of the pure isotope bands, indicating that the ν_3 mode is higher than the ν_1 mode. This is different from OIrO where the ν_1 mode was slightly higher than the ν_3 mode. The ν_1 mode is not infrared active in the linear molecule, but its frequency can be inferred from the position of the $(\nu_1 + \nu_3)$ combination band if present, as in the case of OIrO.[14] This combination band is also found for ORhO, a weak band at 1738.8 cm^{-1}, which tracks with the 900.1 cm^{-1} band under all conditions. The $^{18}O_2$ counterpart for this band is at 1653.2 cm^{-1} to give an isotopic ratio of 1.05178, almost the average of the ratio for ν_3 and ν_1 (predicted to be pure oxygen, 1.06081). An intermediate band is present in the scrambled isotopic experiment at 1699.4 cm^{-1}. Allowing 6.3 cm^{-1} for anharmonicity (see below), the ν_1 frequency is estimated to be 845 cm^{-1}, lower than the ν_3 frequency as expected from the scrambled isotopic data. The ν_1 frequency in $^{18}ORh^{18}O$ is estimated to be 798 cm^{-1} by the same method.

A molecule containing two equivalent oxygen atoms is expected to give a 1:2:1 intensity pattern in the scrambled isotopic experiment. The reduced intensity of the intermediate component for ORhO in the scrambled isotopic experiment is due to coupling between the symmetric and antisymmetric modes in the mixed isotopic molecule $^{16}ORh^{18}O$. The infrared inactive symmetric mode gains intensity through this coupling and is observed at 817.7 cm^{-1} in the scrambled isotopic experiment. The combination band for the mixed molecule $^{16}ORh^{18}O$ is at 1699.4 cm^{-1}, and subtracting this from the sum of the ν_3 and ν_1 frequencies shows that the anharmonicity effect amounts to 6.3 cm^{-1}. This value was used to estimate the ν_1 frequency for the pure isotopic analogues.

The ORhO molecule has been calculated using DFT in both doublet and quartet states, and the results are summarized in Tables 2 and 3. The doublet state is predicted to be the ground state, in agreement with the earlier ESR study of this molecule,[27] and the geometry is calculated to be essentially linear. Mulliken charges are +0.76 on Rh and −0.38 on each O. DFT/D95* fails to give stable linear structures for OCoO, ORhO, and OIrO although ESR spectra and oxygen isotopic ratios indicate linear molecules.[13,14,27] The ν_3 frequency is calculated to be 59.4 cm^{-1} too high, almost identical to the error in the calculated frequency for OIrO. The separation between the ν_1 and ν_3 frequencies is predicted quite accurately, 55.1 cm^{-1} **(**experiment) compared to 71.9 cm^{-1} **(**theory), though not as accurately as for OIrO.[14] The scale factors for ν_3 and ν_1 of ORhO, 0.938 and 0.952, are essentially the same as found for RhO. An earlier UHF calculation for linear ORhO failed to find the bound ground state.[22b]

To test the basis set effects, ORhO was recalculated using the larger 6-311+G(3d) basis set on oxygen, which includes s and p diffuse functions and three sets of d polarization functions. The results of these new calculations are summarized in Table 4. ORhO is calculated to be linear with a $^2\Sigma_g^+$ ground state, in

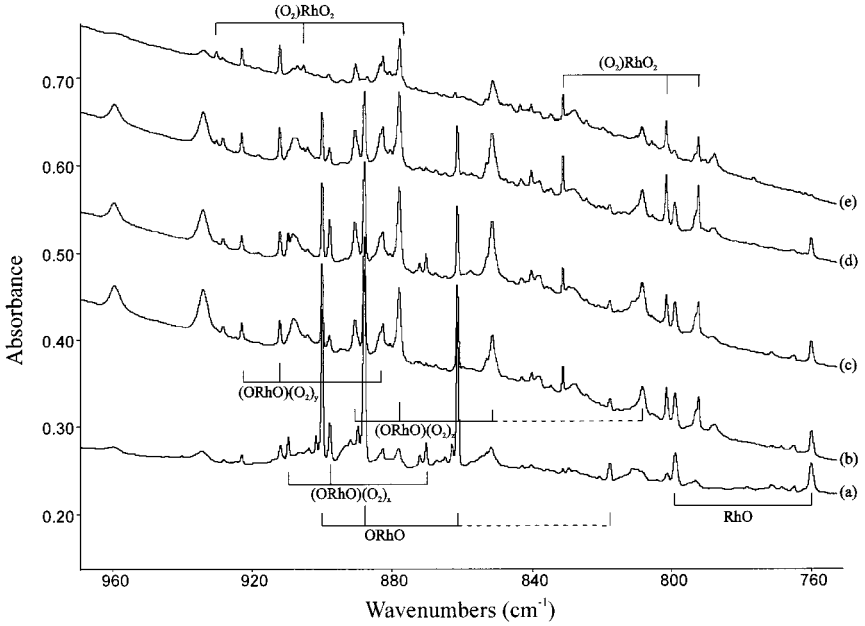

Figure 4. Infrared spectra in the 960−760 cm^{-1} region for laser-ablated rhodium atoms co-deposited with $^{16}O_2+^{16}O^{18}O+^{18}O_2$ in argon (1%) on a 7−8 K window: (a) after 2 h 50 min deposition, (b) after annealing to 35 K, (c) after photolysis for 25 min, (d) after annealing to 40 K, and (e) after annealing to 47 K.

TABLE 1: Infrared Absorptions (cm^{-1}) Observed Following the Codeposition of Laser-Ablated Rhodium Atoms with Oxygen/Argon Mixtures at 7−8 K

$^{16}O_2$	$^{18}O_2$	$^{16}O_2+^{18}O_2$	$^{16}O_2+^{16}O^{18}O+^{18}O_2$	16/18 ratio	assignment
1738.8	1653.2	1738.8, 1653.2	1738.8, 1699.4, 1653.2	1.05178	ORhO
1686.0	1603.5	1686.0, 1603.5	(b)	1.05145	$(O_2)RhO_2$
1367.3	1291.2	1367.3, 1337.5, 1322.4, 1291.2	1367.3, 1337.5, 1322.4, 1291.2	1.05894	OORhO
1280.1	1207.8	1279.4, 1208.7	1279.5, 1244.8, 1208.6	1.05986	$Rh_b(O_2)_z$
1269.6	1198.2	1268.9	1268.5, 1235.2, 1199.1	1.05959	$Rh_b(O_2)_z$
1218.5	1150.1	1217.2, 1158.1	1216.8, 1184.0, 1150.3	1.05947	$Rh_b(O_2)_y$
1215.1	1145.8	1150.0		1.06048	$Rh_b(O_2)_y$
1180.4	1115.3	(a)	(a)	1.05837	$(O_2)RhO$
1131.5	1068.4	(a)	(a)	1.05906	$Rh_c(O_2)_y$
1127.4	1064.4	1127.4, 1064.4	(a)	1.05919	$Rh_c(O_2)_x$
1116.9	1053.5	1115, 1054	1115, 1085, 1054	1.06018	$(ORhO)(O_2)_z$
1090.2	1029.0	(a)	(a)	1.05948	$Rh(O_2)$
1080.4	1019.9	(a)	(a)	1.05932	$Rh_b(O_2)_x$
1076.7	1016.7	(a)	(a)	1.05901	$Rh_b(O_2)_w$
1056.1	997.4	(a)	(a)	1.05858	$(O_2)Rh(O_2)$ site
1048.4	990.3	1048.4, 1002.8, 990.3	(a)	1.05867	$(O_2)Rh(O_2)$
1039.6	982.3	(a)	(a)	1.0583	O_3
1033.1	976.2	(a)	(a)	1.0583	O_3 site
959.7	908.0	959.5, 908.1	959.5, 934.1, 908.1	1.05694	$Rh_x(O_2)_y$
930.3	880.3	930.3, 880.3	930.3, 905.3, 880.3	1.05680	$(O_2)RhO_2$ (site)
928.6	878.6	928.6, 878.6	928.6, 904.2, 878.6	1.05691	$(O_2)RhO_2$
923.0	882.7	923.0, 882.7	923.0, 912.0, 882.7	1.04566	$(ORhO)(O_2)_y$
911.7	872.2	911.7, 872.2	911.7, (obsc.), 872.2	1.04529	$(ORhO)(O_2)_x$ (site)
909.7	870.4	909.7, 870.4	909.7, 897.9, 870.4	1.04575	$(ORhO)(O_2)_x$
903.9	864.9	903.9, 864.9	903.9, 892.0, 864.9	1.04509	ORhO (site)
901.8	863.0	901.8, 863.0	901.8, 889.8, 863.0	1.04495	ORhO (site)
900.1	861.3	900.1, 861.3	900.1, 888.0, 861.3, 817.7	1.04505	ORhO
893.4	854.1	893.4, 854.1	893.4, 880.6, 854.1	1.04601	$(ORhO)(O_2)_z$ (site)
890.7	851.4	890.7, 851.4	890.7, 878.1, 851.4, 808.3	1.04616	$(ORhO)(O_2)_z$
865.4	820.7	(b)	(b)	1.05447	$(O_2)RhO_2$
862.1	824.0	(b)	(b)	1.04623	?
843.4	805.5	(a)	(a)	1.04705	?
831.1	792.2	831.1, 792.2	831.1, 801.3, 792.2	1.04910	$(O_2)RhO_2$
827.1	787.8	827.1, 787.8	(a)	1.04989	$(O_2)RhO_2$ aggregate
819.7	775.9	(a)	(a)	1.05645	aggregate
801.1	764.7	(b)	(b)	1.04760	?
799.0	759.8	799.0, 759.8	799.0, 759.8	1.05159	RhO
728.2	693.1	(a)	728.2, 706.3, 693.1	1.05064	(RhO) complex
622.3	594.0	(a)	(a)	1.04764	aggregate
593.8	564.8	(b)	(b)	1.05135	aggregate
562.4	535.6	562.4, 547.0, 535.6	562.4, 547.0, 535.6	1.05004	Rh_2O_2
473.5	448.4	473.5, 448.4	(b)	1.05598	$(O_2)RhO_2$

[a] Spectral region too congested to identify intermediate components. [b] Pure isotopic bands not present in mixed/scrambled isotopic experiment.

complete agreement with the ESR study on this molecule.[17] This shows that the bent geometry calculated earlier was a consequence of the small basis set rather than the theoretical method used. The ν_1 and ν_3 frequencies are calculated to be 936.6 and 876.7 cm^{-1}, respectively, in closer agreement with experiment. However, the ν_2 frequency is calculated to be −82.9 cm^{-1}, which is clearly incorrect. Thus even with the large basis set on oxygen, the calculation is still flawed. This may be due to the method used or perhaps a deficiency in the valence basis set on rhodium. The Mulliken charges are +1.36 and −0.68 for rhodium and oxygen, larger than with the smaller basis set. Using the larger basis set is expected to improve the charge distribution in the molecule, and these charges are probably more realistic than those calculated using the smaller basis set.

Near the 900.1 cm^{-1} band, three sharp bands at 923.0, 909.7, and 890.7 cm^{-1} exhibit different annealing behavior, with the latter band most prominent. The $^{18}O_2$ counterparts for these bands are at 882.7, 870.4, and 851.4 cm^{-1}, giving 16/18 isotopic ratios of 1.04566, 1.04575, and 1.04616, respectively. These ratios are very close to the ratio for linear ORhO, and these bands correspond to ORhO perturbed by dioxygen in three different ways, suggesting a very slight bending of the O−Rh−O angle. These bands exhibit skewed triplets in the scrambled isotopic experiment with intermediate bands at 912.0, 897.9, and 878.1 cm^{-1}, respectively, analogous to the parent ORhO absorption at 900.1 cm^{-1}. The ORhO bond angles in these complexed forms estimated from the observed isotopic ratios (159°, 157°, and 148°) are only slightly distorted from the linear ORhO geometry. The 909.7 and 923.0 cm^{-1} bands give way to the 890.7 cm^{-1} band, which tracks with the 1116.7 cm^{-1} band on annealing and with more concentrated O_2. This band is assigned to the O−O stretching mode(s) in the higher $(ORhO)(O_2)_z$ complex. Isotopic data for this band demonstrate the primary involvement of one O_2 subunit with secondary coupling to other O_2 molecules. We note the absence of the 900 cm^{-1} band in pure dioxygen,[11,12] which apparently quenches thermal Rh and favors complex formation instead of the insertion reaction.

The bands at 923.0, 909.7, 900.1, and 890.7 cm^{-1} have been observed in a previous matrix isolation study of the reaction of thermal rhodium atoms and dioxygen by Hanlan and Ozin (HO), but were erroneously assigned to the O−O stretching modes of various dioxygen complexes,[11,12] despite the inappropriate oxygen isotopic ratios (1.045) for an O−O stretching mode. In this earlier work the metal atoms were produced thermally, and the fact that ORhO was still observed indicates that the insertion reaction occurs quite readily even with ground-state metal atoms. In fact, it is very interesting to note that the argon matrix spectra

TABLE 2: Calculated (BPW91/D95*/ECP+DZ) States, Geometries, and Relative Energies for Rhodium Oxide Species

molecule	state	(kJ/mol)	$\langle S^2 \rangle$	geometry (Å, deg)
RhO	$^2\Sigma^+$	+30	0.7701	r(Rh−O): 1.740
	$^4\Sigma^-$	0	3.7500	r(Rh−O): 1.739
	$^6\Sigma^-$	+211	8.7500	r(Rh−O): 1.850
ORhO	$^2A_1$	0	0.7500	r(Rh−O): 1.714, ∠ORhO: 155.6
	$^4B_2$	+58	3.7500	r(Rh−O): 1.761, ∠ORhO: 118.3
$ORhO^-$	$^1A_1$	−239	NA	Rh−O: 1.746, ∠ORhO: 161.5
	$^3\Pi_g$	−194	2.0000	Rh−O: 1.790, ∠ORhO: 180.0
$ORhO^+$	$^1A_1$	+954	NA	Rh−O: 1.686, ∠ORhO: 149.5
	$^3B_2$	+1014	2.0001	Rh−O: 1.732, ∠ORhO: 117.8
$Rh(O_2)$	$^2A_2$	+141	0.7500	r(Rh−O): 1.968, r(O−O): 1.340
	$^4B_1$	+194	3.7500	r(Rh−O): 2.127, r(O−O): 1.351
RhOO	^4A	+176	3.7500	r(Rh−O): 1.953, r(O−O): 1.300, ∠RhOO: 112.6
$(O_2)RhO$	$^2B_2$	0	0.8672	$Rh-O_r$: 1.735, $Rh-O_c$: 2.061, O−O: 1.316, $\angle O_cRhO_c$: 37.2, d(ORhOO): 180.0
	$^4B_2$	+12	3.7500	Rh_rO_r: 1.738, $Rh-O_c$: 2.027, O−O: 1.330, $\angle O_cRhO_c$: 38.3, d(ORhOO): 180.0
OORhO	$^2\Sigma_g^+$	+8	0.7711	$Rh-O_r$: 1.714, $Rh-O_c$: 1.831, O−O: 1.259, $\angle O_rRhO_c$: 180.0, $\angle RhO_c^+O_c^+$: 180.0
	$^4A^-$	+71	3.7500	$Rh-O_r$: 1.748, $Rh-O_c$:1.964, O−O: 1.228, $\angle O_rRhO_c$: 133.1, $\angle Rh-O_cO_c$: 132.5
$(O_2)RhO_2$	$^2A_2$	0	0.7500	$r(Rh-O_t)$: 1.734, $r(Rh-O_c)$: 1.953, $r(O_c-O_c)$:1.400, $\angle O_tRhO_t$: 115.2, $\angle O_cRhO_c$: 42.0
	$^4A_1$	+32	3.7501	$r(Rh-O_t)$: 1.734, $r(Rh-O_c)$: 2.244, $r(O_c-O_c)$: 1.313, $\angle O_tRhO_t$: 126.0, $\angle O_cRhO_c$: 34.0
$(OO)RhO_2$	$^2A'$	+11	0.7626	$r(Rh-O_t)$: 1.742, $r(Rh-O_c)$: 1.959, $r(O_c-O_c)$: 1.305, $\angle O_tRhO_t$: 123.0, $\angle RhO_cO_c$: 101.5
	$^4A'$	+15	3.7500	$r(Rh-O_t)$: 1.743, $r(Rh-O_c)$: 2.031, $r(O_c-O_c)$: 1.295, $\angle O_tRhO_t$: 123.8, $\angle RhO_cO_c$: 101.1
$(O_2)Rh(O_2)$ (D_{2d})	$^2B_1$	+18	0.7500	r(Rh−O): 1.953, r(O−O): 1.364, ∠ORhO: 40.9, d(OORhO): 90.0
(D_2)	$^4B_1$	+28	3.7500	r(Rh−O): 2.020, r(O−O): 1.336, ∠ORhO: 38.6, d(OORhO): 41.9
$(O_2)Rh(O_2)$ (D_{2h})	$^2B_{2u}$	+34	0.7835	Rh−O: 2.065, O−O: 1.328, ∠ORhO: 37.5, d(OORhO): 0.0
Rh_2O_2	^1A_g	+28		r(Rh−O): 1.911, ∠RhORh: 93.4, d(ORhRhO): 180.0
	$^3B_{2u}$	+8	2.0000	r(Rh−O): 1.927, ∠RhORh: 80.7, d(ORhRhO): 180.0
	$^5A_1$	0	6.0000	r(Rh−O): 1.943, ∠RhORh: 84.6, d(ORhRhO): 154.5
	$^7B_1$	+87	12.0000	r(Rh−O): 1.987, ∠RhORh: 94.2, d(ORhRhO): 180.0

TABLE 3: Frequencies Calculated (BPW91/D95*/ECP+DZ) for Selected Rhodium Oxide Structures

molecule (state)	calculated frequencies, cm^{-1} (intensities, km/mol)
RhO ($^2\Sigma^+$)	845.1 (49)
RhO ($^4\Sigma^-$)	838.3 (63)
ORhO ($^2A_1$)	959.5 (174), 887.6 (7), 143.8 (8)
$ORhO^+$ ($^1A_1$)	991.2 (94), 929.2 (0), 189.9 (12)
$ORhO^-$ ($^1A_1$)	918.2 (215), 833.0 (11), 121.6 (0)
$Rh(O_2)$ ($^2A_2$)	1112.1 (88), 490.4 (0), 129.7 (12)
$(O_2)RhO$ ($^2B_2$)	1199.3 (126), 864.3 (36), 381.1 (0), 152.4 (5), 131.4 (8), 62.8 (0)
OORhO ($^2\Sigma_g+$)	1430.6 (252), 922.8 (117), 445.5 (0), 354.5 (0), 354.5 (0), 70.4 (4), 70.4 (4)
$(O_2)RhO_2$ ($^2A_2$)	989.4 (98), 882.9 (24), 845.5 (97), 490.0 (0), 423.4 (3)
$(OO)RhO_2$ ($^2A'$)	1182.9 (177), 851.3 (80), 827.7 (44), 520.5 (4)
$(O_2)Rh(O_2)$ ($^2B_1$)	1077.0 (0), 1052.7 (342), 544.2 (8), 438.5 (5), 320.2 (0), 267.2 (8)
$(O_2)Rh(O_2)$ ($^4B_1$)	1131.2 (0), 1117.3 (283), 406.7 (2), 394.5 (1), 392.2 (0), 291.7 (0)
Rh_2O_2 (^1A_g)	652.8 (0), 565.9 (20), 446.4 (0), 406.8 (108), 235.7 (0), 223.6 (25)
Rh_2O_2 ($^3B_{2u}$)	710.9 (0), 568.4 (31), 341.2 (0), 290.6 (0), 276.8 (14), 269.1 (7)
Rh_2O_2 ($^5A_1$)	669.1 (6), 547.9 (18), 330.7 (5), 318.6 (0), 252.4 (0), 91.8 (16)

reported by Hanlan and Ozin[11,12] are very similar to our spectra with the major difference probably arising from their 10−12 K deposition temperature and our colder 7−8 K substrate. For this reason the complex bands reported at 922, 908, and 890 cm^{-1} are much larger relative to the 902 cm^{-1} band,[11,12] which is strong and sharp in the present experiments.

The sharp 900.1 cm^{-1} band is the major product observed here and is clearly due to the isolated ORhO molecule. The formation of ORhO on deposition with thermal Rh atoms but no growth on annealing the cold matrix shows that a small activation energy is required for the insertion reaction 1 to form ORhO. The observation of RhO in addition to using laser-ablated Rh atoms suggests that additional energy is required for abstraction reaction 2.

$$Rh + O_2 \rightarrow ORhO \quad (1)$$

$$Rh^* + O_2 \rightarrow O + RhO \quad (2)$$

The insertion product OMO has been observed for all of the group 9 metals. In each case the molecule is linear, and the ν_3 absorption is the most prominent product band in the spectrum.[13,14] The ν_1 modes are not directly observable but are estimated from the $\nu_1+\nu_3$ combination bands in each system. This provides enough information to calculate the force constants, which are shown in Table 5. The low frequency deformation mode was ignored in these calculations, and simple harmonic motion was assumed. The metal−oxygen bonding as revealed by the force constants clearly becomes stronger moving down the group, increasing by ∼20% per row. This arises because of the increased interaction between the ligand orbitals and the more diffuse d orbitals of the heavier members of the group. This trend is common for transition metal complexes, as reflected by their ligand field splitting parameters, and was also observed for matrix-isolated cobalt and rhodium nitrides.[28−30]

$(O_2)RhO_2$. A sharp band grows in at 831.1 cm^{-1} on annealing and decreases on photolysis. The $^{18}O_2$ counterpart for this band is at 792.2 cm^{-1}, giving an isotopic ratio of 1.04910. This is indicative of the ν_3 mode in a ORhO type molecule but is significantly higher than the value of 1.04505 for linear ORhO, and so cannot be attributed to a form of weakly perturbed ORhO but to a distinct chemical species that contains an ORhO unit. The fact that this species absorbs at a considerably lower frequency than ORhO and its weakly perturbed analogues supports this view. An intermediate band is observed at 801.3 cm^{-1} in the scrambled isotopic experiment to give a 1:1.1:1 intensity triplet. This band is not present initially in the mixed $^{16}O_2+^{18}O_2$ isotopic experiment, but grows in to a small extent on annealing. The intermediate component is 10.4 cm^{-1} *below*

TABLE 4: Geometries and Frequencies Calculated Using the 6-311+G(3d) Basis Set on Oxygen

molecule	electronic state	$\langle S^2 \rangle$	geometry (Å, deg)	frequencies (intensities)	Mulliken populations
ORhO	$^2\Sigma_g+$	0.7500	r(Rh−O): 1.726	936.6 (193)	Rh: +1.36
			∠ORhO: 180.0	876.7 (0)	O: −0.68
$(O_2)RhO_2$	$^2A_2$	0.7500	r(Rh−O_t): 1.738	975.9 (108)	Rh: +1.92
			r(Rh−O_c): 1.952	871.0 (26)	O_t: −0.63
			r(O_c−O_c): 1.396	835.0 (114)	O_c: −0.33
			∠O_tRhO_t: 114.6	503.3 (0)	
			∠O_cRhO_c: 41.9	447.0 (4)	

[a] O_t and O_c denote terminal and cyclic oxygen atoms.

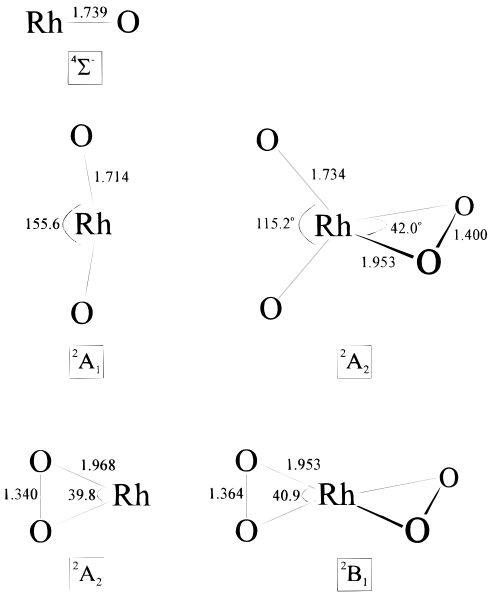

Figure 5. Structures for important rhodium oxide species calculated by BPW91/D95*/ECP+DZ.

TABLE 5: Force Constants (Nm^{-1}) for the Group Nine Metal Oxides OMO and $(O_2)MO_2$

	OMO		$(O_2)MO_2$	
metal	f_{M-O}	$f_{M-O/M-O}$	f_{M-O}	$f_{M-O/M-O}$
Cobalt	530.4	−15.3	535.8	11.8
Rhodium	627.9	45.2	589.5	50.0
Iridium	764.7	50.0	717.6	66.4

the midpoint of the pure isotopic bands, indicating that the ν_3-type mode is lower than the ν_1-type mode. This ordering is the opposite of that observed for isolated ORhO, again showing that the absorbing species is distinct from ORhO. The reduced intensity of the intermediate component also indicates strong coupling between the stretching modes of the $^{16}ORh^{18}O$ unit.

The discussion above regarding ORhO showed that the rhodium−oxygen and iridium−oxygen systems are very similar. In the case of iridium a well-defined dioxygen complex of OIrO was identified, $(O_2)IrO_2$, with the OIrO unit distorted from linear and strongest absorption significantly lower than that for OIrO, corresponding to the ν_3-type mode in the OIrO unit in the complex.[14] This is completely analogous to the 831.1 cm^{-1} band in the rhodium system, which is assigned to the side-bound peroxide complex $(O_2)RhO_2$. Careful examination of the spectra revealed four more bands that track with the 831.1 cm^{-1} band under all conditions, at 1686.0, 928.6, 865.4, and 473.5 cm^{-1}, with $^{18}O_2$ counterparts at 1603.5, 878.6, 820.7, and 448.4 cm^{-1}, respectively. These bands are identified from 16/18 ratios and discussed in turn.

The 865.4 cm^{-1} band is much weaker than the 831.1 cm^{-1} band, has an isotopic ratio of 1.05447, appropriate for a symmetric ORhO motion, and is assigned to the symmetric ORhO stretching mode of $(O_2)RhO_2$. Unfortunately the product yield was low in the scrambled isotopic experiment and this band could not be observed; however, no intermediate band was observed in the mixed isotopic experiment. The bond angle in the ORhO unit can be estimated and is found to be 109° and 113° from the symmetric and antisymmetric 16/18 ratios, respectively. In a simple triatomic molecule these represent the lower and upper limits for the bond angle, but this does not apply when the triatomic is part of a larger molecule.[31] In the case of $(O_2)IrO_2$ the isotopic data for the antisymmetric stretching mode gave the best estimate for the bond angle, but here there is very little difference between them. The relatively weak band at 1603.5 cm^{-1} is the combination band for these stretching modes, and the 10.5 cm^{-1} discrepancy is due to anharmonicity. The $^{16}ORh^{18}O$ isotopic band was obscured and could not be observed. This is analogous to the iridium−oxygen system, where the combination bands for both OIrO and (O_2)-IrO_2 were observed. The rhodium−oxygen system differs in that the O−O stretching mode of the complex is observed at 930.3/928.6 cm^{-1}. These bands are relatively weak; the combined area is only 60% of the 831.1 cm^{-1} band. This suggests that the side-on geometry for the dioxygen group is correct. If it were end-bound to rhodium, the intensity would be much higher, and the band would also lie at a considerably higher frequency, as has been observed in other metal−oxygen systems.[13,16] The dissimilar oxygen atoms in the dioxygen group would also give rise to a splitting of the intermediate component in the scrambled isotopic experiment, but this is not observed. No intermediate bands are observed in the mixed isotopic experiment, but in the scrambled isotopic experiment additional bands are apparent at 905.3/904.2 cm^{-1}. These are only marginally displaced from the midpoint of the pure isotopic bands, indicating that the mode is only weakly coupled to other modes in the complex.

The low-frequency band is due to one of the Rh−O stretching modes within the $Rh(O_2)$ unit. The isotopic ratio of 1.05598 is much larger than the diatomic value and in the case of an acute angle indicates an antisymmetric stretching motion. This band is very weak, having only 4% the intensity of the 831.1 cm^{-1} band. Unfortunately, the expected triplet in the scrambled isotopic experiment could not be observed because of the low product yield; however, the pure isotope bands are observed in the mixed isotopic experiment, but no intermediate band is present. The symmetric $Rh(O_2)$ stretching band was not observed in any experiment.

DFT has been used to calculate the optimum geometry and frequencies of $(O_2)RhO_2$ in doublet and quartet states. The end-bound complex $(OO)RhO_2$ has also been calculated for comparison, and the results are summarized in Tables 2 and 3. As was found for iridium, the doublet state is preferred for both the open and cyclic geometries, which are calculated to have very similar energies. The cyclic geometry is slightly more stable than the asymmetric open form, but the latter is only 11 kJ/mol higher in energy, within the expected error limits for these

calculations. However, the calculated frequencies and intensities show that the end-on geometry must be rejected and that the cyclic geometry is correct. The antisymmetric terminal Rh−O stretching mode is predicted to within 15 cm^{-1} of the experimental value and to be the most intense Rh−O stretching mode. The symmetric Rh−O stretching mode is calculated to within 18 cm^{-1} of the experimental value and to have an intensity only 25% that of the antisymmetric mode, in good agreement with the experimental value of 15%. The O−O stretching mode is predicted to lie 60 cm^{-1} higher than the experimental value and to be as intense as the Rh−O antisymmetric stretching mode. This frequency is reasonable, but the intensity is overestimated by 40%. Overestimation of the intensity for this mode was also found for $(O_2)IrO_2$, where the O−O stretching mode was predicted to have 76% of the intensity of the antisymmetric Ir−O mode but was actually too weak to be observed. Finally, only one of the Rh−O stretching modes within the $Rh(O_2)$ unit is predicted to be observable, with an intensity 3% that of the terminal antisymmetric Rh−O stretching mode. This is almost identical to the intensity observed for this band, and the calculated frequency is within 50 cm^{-1} of the observed value. From these comparisons it is clear that DFT is effective in reproducing the experimental observations for $(O_2)RhO_2$.

The open structure $(OO)RhO_2$ is incompatible with experiment as the O−O stretching frequency is calculated to be over 250 cm^{-1} too high and to have over twice the intensity of the antisymmetric Rh−O stretching mode.

The bond angle of 115.2° calculated for $(O_2)RhO_2$ is in excellent agreement with the value of 109°−113° estimated using the isotopic ratios, and is comparable with the value of 110° calculated for $(O_2)IrO_2$. In the case of iridium the dioxygen ligand was designated a peroxo group on the basis of the calculated partial charges for OIrO and $(O_2)IrO_2$ and the O−O bond length and frequency.[14] The same arguments hold for the rhodium analogue, and $(O_2)RhO_2$ can be considered to be peroxo rhodium dioxide with rhodium approaching the +6 oxidation state. Of course the partial charges are less than the formal oxidation states; the Mulliken charges are +1.08 for Rh, −0.36 for each oxide, and −0.36 for the O_2 unit. The only other example of a Rh(VI) complex is RhF_6. However, it should be noted that the O−O bond length is somewhat longer in (O_2)-IrO_2 than in $(O_2)RhO_2$, 1.444 Å compared to 1.400 Å. Also, the binding energy of O_2 to ORhO is calculated to be 33 kJ/mol, including zero point energy corrections but neglecting BSSE, reaction 3. This is less than half the value of 68 kJ/mol calculated for iridium, indicating a weaker interaction between ORhO and O_2. This can also be deduced experimentally, as is discussed in detail below.

$$ORhO + O_2 \rightarrow (O_2)RhO_2 \ (\Delta E = -33 \text{ kJ/mol}) \qquad (3)$$

The calculation for $(O_2)RhO_2$ was repeated using the 6-311+G-(3d) basis set for oxygen, and the results are summarized in Table 4. The ground state is unchanged, $^2A_2$, and the optimized geometry is almost identical to that obtained using the smaller basis set. The calculated frequencies are in better agreement with experiment, though the symmetric Rh−O and the O−O stretching modes are still erroneously predicted to be strongly coupled, the latter mode having an anomalously high intensity. The Mulliken charges are calculated to be +1.92, −0.63, and −0.33 for rhodium and the terminal and cyclic oxygen atoms, respectively, considerably larger than with the smaller basis. However, the relationship between the atomic charges in ORhO and $(O_2)RhO_2$ is unchanged with the larger basis set. Finally, the energy change for the addition of O_2 to ORhO is calculated to be −62 kJ/mol, almost double the value calculated using the smaller basis set on oxygen. (A similar doubling in O_2-IrO_2 bond strength was also calculated with the larger basis set.) These results show that using the larger basis set gives frequencies in better agreement with experiment and significant improvements in the charge distributions and binding energy. However, the molecular parameters calculated for ORhO and $(O_2)RhO_2$ using the smaller basis set are adequate in determining the extent of the interaction between ORhO and O_2.

The peroxo complex was far more abundant in the iridium system, where $(O_2)IrO_2$ and OIrO were the most prominent reaction products; OIrO was present initially, but was replaced on annealing by $(O_2)IrO_2$. In the case of rhodium, the 901.1 cm^{-1} band of ORhO is by far the most abundant initially, which then decreases rapidly on annealing. The 831.1 cm^{-1} band due to $(O_2)RhO_2$ does grow in but is dwarfed by absorptions of the weaker oxygen complexes of ORhO at 923.0, 909.7, and 890.7 cm^{-1}. Thus while rhodium atoms have a strong affinity for oxygen, this is not as strong as for iridium and ORhO does not form the defined peroxo complex as readily. The cobalt−oxygen system continues this trend, where a greater variety of species are formed on annealing and $(O_2)CoO_2$ is only a minor product.[13,14]

The effect of binding O_2 to the OMO insertion product (M = Co, Rh, Ir) can be quantified by calculating the force constants of the M−O bonds within the OMO unit and comparing them to the values obtained for uncomplexed OMO. The stronger the interaction between OMO and O_2, the greater the change in the M−O bond strengths will be. In these calculations the OMO unit is considered in isolation, and the bond angles are assumed to be that estimated from the isotopic ratio for the antisymmetric stretching mode which are 130°, 113°, and 108° for cobalt, rhodium, and iridium, respectively. The force constants for these molecules are compared in Table 5. Both rhodium and iridium show a decrease in the strength of the M−O terminal bonds, by 47.1 Nm^{-1} and 38.4 Nm^{-1}, respectively, indicating a significant interaction between OMO and the complexed dioxygen group. The decrease is greater for iridium, consistent with the above discussion. By contrast the force constant increases by 5.4 Nm^{-1} for the cobalt analogue. This is probably within the error of the calculation and indicates that the interaction between OCoO and O_2 is weak, as discussed above. Another parameter which seems to indicate the extent of interaction between the insertion product OMO and O_2 is the bond angle, which is linear in the isolated molecule but becomes distorted when complexed to O_2. The distortion is large for rhodium and iridium, with that for iridium being marginally greater, but is less significant for cobalt. This behavior parallels the changes in the force constants on complexation and supports the view that the metal−dioxygen interactions become stronger moving down the cobalt group. The increasing strength of the interaction with oxygen is consistent with the observation that higher oxidation states are more stable for the second and third row transition metals than for the first row. Thus, cobalt cannot support a +6 oxidation state and so OCoO is only weakly complexed to O_2 in what should be considered a Co(IV) species. By contrast rhodium and iridium form well defined, albeit weakly bound, dioxygen adducts with ORhO and OIrO which are legitimate Rh(VI) and Ir(VI) complexes, with the bonding being stronger in the latter case. This trend is also found in Co^{II} and Rh^{II} complexes.[4]

Rh_2O_2. A weak band is observed at 562.4 cm^{-1} on deposition that grows in strongly on early annealing but decreases on later annealing and is completely destroyed on photolysis. The $^{18}O_2$ counterpart for this band is at 535.6 cm^{-1} to give an isotopic ratio of 1.05004, slightly lower than the diatomic value of

1.05185. A 1:2:1 intensity triplet is observed in the scrambled isotopic experiment, with the intermediate component at 547.0 cm^{-1}. This band is not present initially in the mixed isotopic experiment but grows in slightly on annealing, which shows that two oxygen atoms are involved, and that both come from the same dioxygen molecule. These bands are too low for terminal Rh−O stretching modes, and so bridged and cyclic species must be considered. As is discussed below, there is evidence for several rhodium−dioxygen complexes, and the 562.4 cm^{-1} band could correspond to a Rh−(O_2) stretching mode. However, calculations place this mode below 500 cm^{-1}. Another alternative assignment is to the rhombic ring, Rh_2O_2, which has been observed in numerous metal−oxygen systems including cobalt and nickel.[13,32] The deviation of the isotopic ratio from the expected harmonic diatomic value can be attributed to anharmonicity. The intermediate band at 547.0 cm^{-1} grows in weakly on annealing in the mixed isotopic experiment, but not as rapidly as the pure isotopic peaks. This shows that Rh_2O_2 is formed primarily by the addition of rhodium atoms to Rh(O_2), although dimerization of RhO occurs to a small extent.

DFT has been used to calculate Rh_2O_2 in singlet, triplet, quintet, and septet states, and the results are summarized in Tables 2 and 3. The quintet state is lowest in energy, with the triplet and singlet states higher by only 8 and 27 kJ/mol, respectively. The quintet state is optimized to a nonplanar geometry, and the modes originating from the b_{3g} and a_g stretching modes in a planar ring have nonzero intensity through the dipole moment change perpendicular to the plane of the ring. From the predicted intensities and the observed intensity of the 562.4 cm^{-1} band, these modes should be observable, and their absence disqualifies the quintet state. However, the calculated frequencies for the singlet and triplet states are both compatible with experiment. In these states the molecule is planar, and only one stretching mode is predicted to have observable intensity. The predicted frequencies of 565.9 cm^{-1} and 568.4 cm^{-1} for the singlet and triplet states are both in excellent agreement with the observed 562.4 cm^{-1} band. In the singlet state another infrared active mode is predicted at 406.8 cm^{-1}, which is not observed, but this band may fall below the instrumental limit of 400 cm^{-1}. However, the triplet state is the lowest in energy of the two and is most likely to be the ground state.

(O_2)RhO and OORhO. Weak bands at 1367.3 and 1180.4 cm^{-1} exhibit different growth rates on annealing and 16/18 ratios for O−O stretching modes. The 1367.3 cm^{-1} band is in a cleaner region and the quartets with mixed *and* scrambled isotopic precursors show that the two stretching O atoms are not equivalent. Hence, assignment to OORhO follows with support of the DFT calculation of a strong band at 1430.6 cm^{-1} (scale factor 0.956). The 1180.4 cm^{-1} band is favored on annealing and is assigned to the more stable (O_2)RhO isomer, which has its strongest absorption calculated at 1119.3 cm^{-1} (scale factor 0.984). No other modes were observed for either of these oxide complexes. Similar oxide complexes have been identified with Co and Ni.[13,32]

$Rh_x(O_2)_y$. Over 10 bands are observed in the 1280−960 cm^{-1} region (Table 1), with oxygen isotopic ratios appropriate for O−O stretching modes (near 1.059). These are undoubtedly due to various dioxygen complexes of rhodium atoms and small clusters as it has been shown that Rh atoms have an unusual propensity to form clusters.[11,33] Most of these bands were originally assigned by HO to specific dioxygen clusters,[11,12] but the present observations show that many of the original assignments are incorrect. Unfortunately the mixed and scrambled isotopic data are poor in this region and few definitive assignments can be made. However, several generalizations can be drawn. Some of these bands are sharp (1048.4, 1076.8, 1090.2, 1127.4 cm^{-1}) and others are broad (959.7, 1080.4, 1116.9, 1218.5, 1280.1 cm^{-1}). On annealing (Figure 2) these bands reach maximum intensity at different temperatures, which gives an indirect measure of the degree of reagent aggregation and resulting cluster size. The first sharp band to maximize was 1090.2 cm^{-1} (25 K), followed by 1048.4 cm^{-1} (35 K), then 1076.7 and 1127.4 cm^{-1} (45 K); the broader bands maximized at higher temperatures, 959.7 (25−35 K) 1116.9 cm^{-1} (40 K, tracks with 890.7 cm^{-1}) and 1080.4, 1218.5, 1280.1 cm^{-1} (final 47 K).

To contrast the spectra in Figure 2 (0.6% O_2 with higher laser energy), an experiment was done with 2% O_2 and lower laser energy, thus the O_2/Rh ratio was *increased* by a factor of 5 ± 1. The 1116.9, 1048.4, and 959.7 cm^{-1} bands are favored in the 2% O_2 experiment; the 1076.7, 1080.4, 1218.5, and 1280.1 cm^{-1} bands are disfavored; and the 1131.5 and 1127.4 cm^{-1} bands are eliminated. This suggests that the latter bands have the highest number of Rh atoms, and in agreement with HO, we suggest that these bands involve three Rh atoms, but the small number of O_2 units cannot be determined. The 1116.9 cm^{-1} band has been assigned to the most oxygen-rich species observed here, $(ORhO)(O_2)_z$.

The sharp 1048.4 cm^{-1} band shows definitive mixed and scrambled isotopic data,[11,12] and HO assign a 1048 cm^{-1} band in solid argon to (O_2)Rh(O_2). We agree with this assignment as the triplet absorption observed here with $^{16}O_2+^{18}O_2$ is in accord with their spectrum. In addition our DFT calculation predicts an essentially D_{2d} structure only 18 kJ/mol higher than the (O_2)-RhO_2 complex observed here at 831.1 cm^{-1}. The (O_2)Rh(O_2) molecule has a very strong antisymmetric O−O stretching frequency calculated at 1052.7 cm^{-1}, in excellent agreement with the observed absorption. The Mulliken charges are +0.66 on Rh and −0.33 on each dioxygen unit, which suggests that (O_2)Rh(O_2) is between a disuperoxo and diperoxo species. This (O_2)Rh(O_2) complex is analogous to the Pd and Pt complexes reported previously.[34]

$$O_2 + Rh(O_2) \rightarrow (O_2)Rh(O_2)\ (\Delta E = -147\ kJ/mol) \quad (4)$$

The sharp, weak 1090.2 cm^{-1} absorption reaches maximum intensity early in the annealing cycles (25 K) and this is our best candidate for cyclic Rh(O_2). Recall that the previous[11,12] assignment to Rh(O_2) at 908 cm^{-1} is here identified as (ORhO)-(O_2) because the 16/18 isotopic ratio (1.045) is *too low* for an O−O stretching mode; in our experiment the 909.7 cm^{-1} band is a satellite O_2 complex of the strong ORhO absorption at 900.1 cm^{-1}. It is noteworthy that the relative absorbance of the 1048.4 to 1090.2 cm^{-1} bands with 0.6% O_2 (Figure 1) is 3.5, and with 2% O_2 this ratio increases to 10, which clearly indicates that the 1090.2 cm^{-1} absorber contains *less* O_2 than (O_2)Rh(O_2). The present DFT calculation predicts a strong 1112.1 cm^{-1} O−O stretching mode for the $^2A_2$ ground-state Rh(O_2) complex. On the basis of the above evidence, the 1090.2 cm^{-1} band is assigned to Rh(O_2); the scale factor, 0.980, is appropriate for this density functional.[21]

The broad 959.7 cm^{-1} band is decreased on photolysis and destroyed on the highest annealing (Figure 1). This feature shows a broadened triplet with scrambled isotopic precursor with evidence for a minor secondary isotopic interaction. It can only be identified as $Rh_x(O_2)_y$ with both *x* and *y* low; a possibility is $(Rh(O_2))_2$ but we cannot be certain.[35]

The 1076.7, 1080.4, 1218.5, and 1280.1 cm^{-1} bands share the common behavior that they are disfavored with 2% O_2 and *less* laser power than the 0.6% O_2 sample in Figure 2. This means that these absorbers contain more metal atoms than $(O_2)Rh(O_2)$, and thus these are likely to be dirhodium complexes, in agreement with HO, but we disagree on the number of complexing O_2 subunits. While the 1278 cm^{-1} band assigned to $RhRh(O_2)$ by HO gives a triplet scrambled isotopic spectrum, it is a *broad* triplet, and here the "$^{16}O_2$" and "$^{18}O_2$" counterparts are broadened by 25% and shifted 1 cm^{-1} to the center, which clearly indicates *weak coupling to other O_2 subunits*. Similar behavior is found for the 1218.5 cm^{-1} band. These bands are identified in Table 1 as $Rh_b(O_2)_{w,x,y,z}$; we believe that $b = 2$ and that the number of O_2 ligands probably increases from the sharp 1076.7 cm^{-1} band to the broader 1280.1 cm^{-1} feature (possibly one to four), but we cannot identify specific numbers of O_2 subunits. Recall that HO observed a strong counterpart of the 1280.1 cm^{-1} band at 1266 cm^{-1} *in pure* oxygen.[12]

Owing to the propensity of Rh to form clusters,[11] a large number of $Rh_x(O_2)_y$ complexes are produced. Although many of the earlier assignments[11,12] to specific complexes are incorrect, the more general assignment to $Rh_x(O_2)_y$ complexes is correct. In addition, the HO assignment to $(O_2)Rh(O_2)$ at 1048.4 cm^{-1} is supported by the present DFT frequency calculations and concentration behavior. A new 1090.2 cm^{-1} band is assigned to $Rh(O_2)$ in agreement with DFT calculations.

Other Absorptions. Since previous experiments with laser-ablated metal atoms and dioxygen have produced charged species,[36,37] the spectra were examined accordingly. With the laser power required for Rh ablation, the yield of charged species is typically low, but O_4^+ and O_4^- were detected at 1118.4 and 953.8 cm^{-1}, respectively.[38,39] Calculations were done for $ORhO^+$ and $ORhO^-$ to aid in identification, but no bands were found which could be assigned to charged metal oxide species.

Finally, a higher complex $Rh(O_2)_3$ was considered, as four dioxygen units have been observed in the $Cr(O_2)_4^{3-}$ and $Mo(O_2)_4^{2-}$ anions.[40] Our DFT calculations find a stable doublet (C_3, Rh−O: 2.092, 2.079 Å, O−O: 1.310 Å) and a stable quartet (D_3, Rh−O: 2.084 Å, O−O: 1.310 Å) 2 kJ/mol higher in energy and each has a strong degenerate mode at 1200 ± 1 cm^{-1}. No band was observed near 1200 cm^{-1} that could be associated with this oxygen-rich species and no such band was observed in pure dioxygen.[11] Distortion of $(O_2)Rh(O_2)$ may require more activation energy than is available for reaction 5 in the matrix.

$$(O_2)Rh(O_2) + O_2 \rightarrow Rh(O_2)_3 \ (\Delta E = -44 \text{ kJ/mol}) \quad (5)$$

Conclusions

Laser-ablated rhodium atoms were reacted with dioxygen, and several oxide products were formed including RhO, ORhO, $(O_2)RhO_2$, Rh_2O_2, and a large number of dioxygen complexes. The insertion product ORhO was the most prominent band in the spectrum; this molecule was determined to be linear from the 16/18 isotopic ratio (1.04505), in agreement with a previous ESR study of the molecule.[27] The geometry and frequencies for ORhO were calculated using DFT (BPW91/D95* and 6-311+G(3d)/ECP+DZ). This species is readily complexed by O_2 giving three weakly perturbed nearly linear ORhO complexes and the well-defined peroxo rhodium dioxide $(O_2)RhO_2$ with four stretching modes identified. This is analogous to the iridium−oxygen system in which the primary reaction product OIrO was readily complexed by oxygen to give $(O_2)IrO_2$. Consideration of the calculated parameters for the rhodium complex shows that rhodium is in the +6 oxidation state, also analogous to iridium. However, the interaction with dioxygen is greatest for iridium as shown by the calculated binding energy and the effect of dioxygen binding on the Rh−O and Ir−O force constants in ORhO and OIrO. Reference to the cobalt−oxygen system shows that dioxygen complexation of OCoO is not as significant, and the OCoO molecule is only weakly perturbed. The increasing affinity of OMO for dioxygen moving down the cobalt group is consistent with the increasing stability of higher oxidation states.

The 1280−960 cm^{-1} region contains over 10 bands that are clearly due to a family of side-bound complexes, $Rh_x(O_2)_y$, but in disagreement with previous workers,[11,12] most of these complexes cannot be definitively identified. However, one of the original assignments, $(O_2)Rh(O_2)$ at 1048 cm^{-1} in solid argon, shows the definitive mixed isotopic spectrum for two equivalent dioxygen molecules,[11] and the present experiments and DFT calculations confirm this assignment to the similar D_{2d} structure proposed[11,34] for $(O_2)Pd(O_2)$. In addition, a weak 1090 cm^{-1} absorption behaves appropriately for assignment to $Rh(O_2)$, and our DFT calculations predict a $^2A_2$ ground state with 1112 cm^{-1} O−O stretching frequency. In marked contrast, Co appears to form a family of end-bound complexes[13] and Ir reacts to form OIrO rather than dioxygen complexes.[14]

Acknowledgment. We thank the National Science Foundation (CHE 97-00116) for financial support.

References and Notes

(1) Potter, W. T.; Tucker, M. P.; Houtchens, R. A.; Caughey, W. S. *Biochemistry* **1987**, *26*, 4699.

(2) Hirota, S.; Ogura, T.; Appleman, E. H.; Shinzawa-Itah, K.; Yoshikawa, S.; Kitagawa, T. *J. Am. Chem. Soc.* **1994**, *116*, 10564 and references therein Hirota, S.; Ogura, T.; Kitagawa, T. *J. Am. Chem. Soc.* **1995**, *117*, 821.

(3) Geoffrey, G. L.; Keeney, M. E. *Inorg. Chem.* **1977**, *16*, 205.

(4) Wayland, B. B.; Newman, A. R. *Inorg. Chem.* **1981**, *20*, 3093.

(5) Raynor, J. B.; Gillard, R. D.; Pedrosa de Jesus, J. D. *J. Chem. Soc., Dalton Trans.* **1982**, 1165.

(6) Schwartz, J. *J. Acc. Chem. Res.* **1985**, *18*, 302. Fischer, H. E.; Schwartz, J. *J. Am. Chem. Soc.* **1989**, *111*, 7644.

(7) Crabtree, R. H. *Chem. Rev.* **1985**, *85*, 245.

(8) Patai, S. *The Chemistry of Peroxides*; John Wiley & Sons: New York, 1983. Jorgensen, K. A. *Chem. Rev.* **1989**, *89*, 431.

(9) Reddy, B. V.; Khanna, S. N.; Dunlap, B. I. *Phys. Rev. Lett.* **1993**, *70*, 3323. Reddy, B. V.; Nayak, S. K.; Khanna, S. N.; Rao, B. K.; Jena, P. *Phys. Rev. B* **1999**, in press, and references therein.

(10) Cox, A. J.; Louderback, J. G.; Apsel, S. E.; Bloomfield, L. A. *Phys. Rev. B.* **1994**, *49*, 12295.

(11) Hanlan, A. J. L.; Ozin, G. A. *Inorg. Chem.* **1977**, *16*, 2848.

(12) Hanlan, A. J. L.; Ozin, G. A. *Inorg. Chem.* **1977**, *16*, 2857.

(13) Chertihin, G. V.; Citra, A.; Andrews, L.; Bauschlicher, C. W., Jr. *J. Phys. Chem. A* **1997**, *101*, 8793, (Co+O_2).

(14) Citra, A.; Andrews, L. *J. Phys. Chem. A* **1999**, in press. (Ir+O_2).

(15) Hassanzadeh, P.; Andrews, L. *J. Phys. Chem.* **1992**, *96*, 9177.

(16) Chertihin, G. V.; Saffel, W.; Yustein, J. T.; Andrews, L.; Neurock, M.; Ricca, A.; Bauschlicher, C. W., Jr. *J. Phys. Chem.* **1996**, *100*, 5261.

(17) Frisch, M. J.; Trucks, G. W.; Schlegel, H. B.; Gill, P. M. W.; Johnson, B. G.; Robb, M. A.; Cheeseman, J. R.; Keith, T.; Petersson, G. A.; Montgomery, J. A.; Raghavachari, K.; Al-Laham, M. A.; Zakrzewski, V. G.; Ortiz, J. V.; Foresman, J. B.; Cioslowski, J.; Stefanov, B. B.; Nanayakkara, A.; Challacombe, M.; Peng, C. Y.; Ayala, P. Y.; Chen, W.; Wong, M. W.; Andres, J. L.; Replogle, E. S.; Gomperts, R.; Martin, R. L.; Fox, D. J.; Binkley, J. S.; Defrees, D. J.; Baker, J.; Stewart, J. P.; Head-Gordon, M.; Gonzalez, C.; Pople, J. A. *Gaussian 94, Revision B.1* Gaussian, Inc.; Pittsburgh, PA, 1995.

(18) Becke, A. D. *Phys. Rev. A* **1988**, *38*, 3098.

(19) Perdew, J. P.; Wang, Y. *Phys. Rev. B* **1992**, *45*, 13244.

(20) Hay, P. J.; Wadt, W. R. *J. Chem. Phys.* **1985**, *82*, 299.

(21) Bytheway, I.; Wong, M. W. *Chem. Phys. Lett.* **1998**, *282*, 219.

(22) (a) Mains, G. J.; White, J. M. *J. Phys. Chem.* **1991**, *95*, 112. (b) Siegbahm, P. E. M. *Chem. Phys. Lett.* **1993**, *201*, 15.

(23) (a) Raziunas, V.; Macur, G.; Katz, S. *J. Chem. Phys.* **1965**, *43*, 1010. (b) Norman, J. H.; Staley, H. G.; Bell, W. E. *Adv. Chem. Ser.* **1968**, *72*, 101.

(24) Balfour, W. J.; Fougere, S. G.; Qian, C. X. W., work in progress.

(25) Li, X.; Wang, L.-S. *J. Chem. Phys.* **1998**, *109*, 5264.

(26) (a) Wilson, E. B., Jr.; Decius, J. C.; Cross, P. C. *Molecular Vibrations; The Theory of Infrared and Raman Vibrational Spectra*; McGraw-Hill: New York, 1955. (b) Allavena, M.; Rysnik, R.; White, D.; Calder, V.; Mann, D. E. *J. Chem. Phys.* **1969**, *50*, 3399.

(27) Van Zee, R. J.; Hamrick, Y. M.; Li, S.; Weltner, W., Jr. *J. Phys. Chem.* **1992**, *96*, 7247.

(28) Cotton, F. A.; Wilkinson, G. *Advanced Inorganic Chemistry*, 5th ed; Wiley: New York,1988.

(29) Andrews, L.; Citra, A.; Chertihin, G. V.; Bare, W. D.; Neurock, M. *J. Phys. Chem. A* **1998**, *102*, 2561.

(30) Citra, A.; Andrews, L. *J. Phys. Chem. A* **1999**, *103*, 3410, (RhN).

(31) Hope, E. G.; Levason, W.; Ogden, J. S.; Tajik, M. *J. Chem. Soc., Dalton Trans.* **1986**, *8*, 1587.

(32) Citra, A.; Chertihin, G. V.; Andrews, L.; Neurock, M. *J. Phys. Chem. A* **1997**, *101*, 3109.

(33) Ozin, G. A.; Hanlan, A. L. J. *Inorg. Chem.* **1979**, *18*, 1781.

(34) Huber, H.; Klotzbhcher, W.; Ozin, G. A.; Vander Voet, A. *Can. J. Chem.* **1973**, *51*, 2722.

(35) In an appendix,[11] HO associate 1020 and 960 cm^{-1} bands with nitrogen impurity and a 2280 cm^{-1} band. We do not observe the 1020 cm^{-1} band, and a very weak 2229.2 cm^{-1} band decreases on annealing and *does not track* with our 959.7 cm^{-1} band. Hence, our 959.7 cm^{-1} band does not appear to involve N_2. Furthermore, the 663 cm^{-1} CO_2 band is very weak (0.005 au), and this trace impurity probably does not contribute to our reaction products.

(36) Chertihin, G. V.; Andrews, L. *J. Phys. Chem.* **1995**, *99*, 6356.

(37) Zhou, M. F.; Andrews, L. *J. Phys. Chem. A* **1998**, *102*, 8251.

(38) Chertihin, G. V.; Andrews, L. *J. Chem. Phys.* **1998**, *108*, 6404.

(39) Zhou, M. F.; Hacaloglu, J.; Andrews, L. *J. Chem. Phys.* **1999**, *110*, 9450.

(40) Cundari, T. R.; Zerner, M. C.; Drago, R. S. *Inorg. Chem.* **1988**, *27*, 4239.